^{192}Pt(α,α') reaction at $E = 24$ MeV

F. Todd Baker and Alan Scott
Department of Physics, University of Georgia, Athens, Georgia 30602*

R. M. Ronningen†
Department of Physics, Vanderbilt University,‡ Nashville, Tennessee 37235
and Oak Ridge National Laboratory,§ Oak Ridge, Tennessee 37830

T. H. Kruse and R. Suchannek
Department of Physics, Rutgers University,¶ New Brunswick, New Jersey 08903

W. Savin
Department of Physics, New Jersey Institute of Technology, Newark, New Jersey 07102
(Received 6 July 1977)

Angular distributions for excitation of the 0^+, 2^+, $2^{+\prime}$, 4^+, $4^{+\prime}$, and 3^- states in ^{192}Pt by 24 MeV α particles have been measured. Coupled-channels analysis of the ground-state band yields negative β_4 deformations. Analysis of the "γ band" yields a negative $E2$ interference term P_3 and a surprising large direct $E4$ excitation of the $4^{+\prime}$ state.

[NUCLEAR REACTIONS ^{192}Pt(α,α'), $E_\alpha = 24$ MeV; measured $\sigma(\theta, E'_\alpha)$; deduced Coulomb and nuclear deformations β_2, β_4, β_3, and relative signs of matrix elements. Enriched target. Coupled-channels analysis.]

I. INTRODUCTION

There has recently been much interest in studying the properties of the heavy transitional nuclei ($180 \lesssim A \lesssim 200$). α-particle Coulomb-nuclear interference has been a particularly valuable technique for studying the $E4$ (Refs. 1–6) and $E2$ (Ref. 7) properties of these nuclei. These experiments have employed excitation functions to examine the dependence of the excitation probabilities on the "distance of closest approach" of the α particles.

In the experiment described here we have extended these measurements to the nucleus ^{192}Pt. This nucleus is of particular interest because it lies in the "heart" of the region where the prolate-oblate transition occurs. It is also the lightest Pt isotope for which it is practical to obtain a target. The present experiment differs from previous Coulomb-nuclear interference studies in that angular distributions at a fixed energy (24 MeV) were used to determine the distance of closest approach dependence of the excitation probabilities. We find this technique to be more convenient than the excitation function method, both experimentally and from the standpoint of ease of analysis.

II. EXPERIMENTAL DETAIL

α particles were accelerated by the Rutgers-Bell FN tandem to an energy of 24 MeV. Typical beam intensity on target was 1 μA. The scattered α particles were detected in a position-sensitive proportional counter placed on the image surface of the split-pole spectrograph.

The target was approximately 20 μg/cm^2 of $\gtrsim 99\%$ isotopically enriched ^{192}Pt deposited on an 80 μg/cm^2 carbon backing in an isotope separator.

Absolute cross sections were determined by measuring the 25°–130° elastic-scattering yields relative to a monitor detector placed at 45° in a conventional scattering chamber. The overall normalization was determined by equating small-angle data to the Rutherford scattering cross section. The spectrograph data were then normalized to the cross sections determined in the scattering chamber.

An energy level diagram showing the states most strongly excited is shown in Fig. 1.

III. ANALYSIS TECHNIQUES

The data were analyzed using the coupled-channels code ECIS.[8] Calculations included 80 partial waves and integrations were performed to 50 fm; these limits were found to be more than adequate for the angular range of the data.

The optical-model parameters were determined by simultaneously fitting elastic and inelastic scattering cross sections during the analysis of the ground-state band transitions described below. The optical potential assumed was a four-parameter potential with $r_0 = 1.44$ fm, $a = 0.605$ fm, $W = 11.2$ MeV; data were fitted by simultaneously varying the real well depth and the coupling

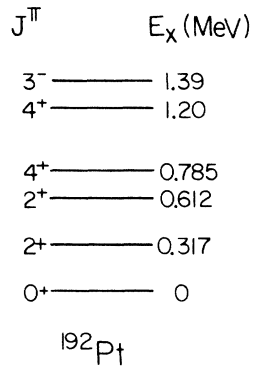

FIG. 1. Energy level diagram of ^{192}Pt showing the states most strongly excited by the (α,α') reaction at 24 MeV.

strengths. The resulting parameters, shown in Table I, were used for all other calculations and provided excellent fits to the elastic scattering data throughout. Recent results[9,10] for elastic scattering of 142 MeV α particles have determined that a substantially deeper real potential ($V \simeq 120$ MeV) is the correct α-particle-nucleus interaction and that a six-parameter potential with geometry quite different from that of our potential is required. We have elected to use the simpler four-parameter potential for several reasons: (i) most importantly, we wish to facilitate comparison of our results with previous experiments[1-7] in this target mass, projectile energy region, all of which have used an optical potential more similar to ours; (ii) since the projectile, being strongly absorbed, does not sample the interior regions of the potential at $E_\alpha = 24$ MeV, the potential need only be well represented near and outside the strong-absorption radius and the excellent fit to our elastic data (Fig. 2) is indicative that this requirement has been met; (iii) uncertainties about the energy dependence of the potential of Refs. 9 and 10 as well as the uncertain effects of explicit coupling on this potential made its use less attractive when applied to the relatively low-energy α particles used in the present experiment.

The form factors and relative matrix elements used in the calculations will be described in the subsections of Sec. IV since they differ significantly for states of differing character.

It should be noted here, from a practical viewpoint, that angular distribution data are much easier to analyze than excitation function data. It has therefore been possible to perform analysis for states which, because of limitations on computing time, are generally left unanalyzed in excitation-function experiments.

TABLE I. Optical-model parameters.

V (MeV)	W (MeV)	r_0 (fm)	a (fm)	r_0^c (fm)
40.5	11.2	1.44	0.605	1.20

IV. EXPERIMENTAL RESULTS AND DISCUSSION

A. Ground-state band transitions

The data for excitation of the 0^+, 2^+, 4^+ members of the ground-state band were analyzed using rotational-model form factors. All matrix elements, with the exception of the reorientation matrix elements, were assumed to be those of a simple rotor. This is in accord with the recent lifetime measurements of Johnson *et al.*[11] Since the quadrupole moments of the 2^+ and 4^+ states have not been measured, all reorientation matrix elements were assumed to have half the oblate rotational-model values. This estimate was made by examining the systematics of the measured[12,13] quadrupole moments of ^{194,196,198}Pt; the results of the calculations, however, were quite insensitive to this assumption.

The four deformation parameters (β_2^C, β_4^C, β_2^N, β_4^N) were then varied in an automatic search on the data for the 2^+ and 4^+ states. The results of this search are shown in Table II; the fits to the data are shown in Fig. 2. The qualitative features of the 4^+ data, notably the interference minimum near 80°, allow an unambiguous determination of the signs of the β_4 deformations. The signs of the β_2 deformations are not unambiguously determined by the data and equally good fits could probably be achieved assuming $\beta_2 > 0$. ^{192}Pt is expected to have an oblate intrinsic shape and our negative β_2 is the result of starting the search with $\beta_2 < 0$.

Also shown in Table I are the reduced transition rates $B(E2; 0^+ \to 2^+)$ and $B(E4; 0^+ \to 4^+)$. These were

TABLE II. Spectroscopic results for ground-state band transitions.

β_2^C [a]	−0.180
β_4^C [a]	−0.079
β_2^N [a]	−0.152
β_4^N [a]	−0.033
$\beta_2^{N'}$ [b]	−0.142
$\beta_4^{N'}$ [b]	−0.065
$B(E2, 0^+ \to 2^+)$ [c]	$1.92\, e^2\text{b}^2$
$B(E4, 0^+ \to 4^+)$ [c]	$0.041\, e^2\text{b}^4$

[a] Estimated uncertainty of ±10%.
[b] Predicted by the Hendrie scaling procedure (Ref. 13).
[c] Deduced using Eqs. (1) and (2) of the text.

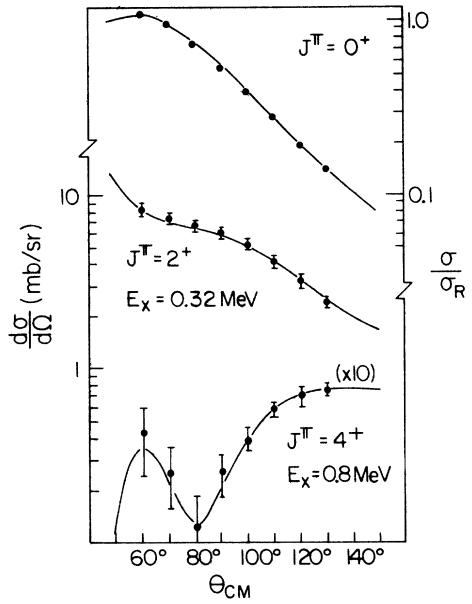

FIG. 2. Data and coupled-channels fits for the 0^+, 2^+, 4^+ members of the ground-state band. The fits, described in detail in Sec. IV A of the text, used parameters given in Tables I and II.

calculated by evaluating numerically the integrals

$$[B(E\lambda; 0^+ \to \lambda^\pi)]^{1/2} = \int \rho(r,\theta) r^\lambda Y_{\lambda_0}(\theta) d\tau \qquad (\lambda = 2, 4). \quad (1)$$

The charge density $\rho(r,\theta)$ used in this calculation was that of a uniform deformed charge distribution with the surface parametrized by

$$R(\theta) = 1.2 \times 192^{1/3}[1 + \beta_2^C Y_{20}(\theta) + \beta_4^C Y_{40}(\theta)]. \quad (2)$$

This is the same charge distribution which was used to compute the Coulomb-excitation form factors in the coupled-channels calculations. The $B(E2)$ value determined here is in good agreement with the recent Coulomb-excitation results of Ronningen *et al.*[14] (1.89 ± 0.03 e^2b^2) even though the present experiment was performed above the Coulomb barrier and none of the data are at a small enough angle to have negligible nuclear-excitation contributions.

The value of β_2^N is in good agreement with the value expected (labeled $\beta_2^{N'}$ in Table II) assuming that β_2^C represents an "intrinsic" quadrupole deformation and that the Hendrie scaling procedure[15] accounts for the nonzero projectile size. This procedure, however, fails to account for the rather large discrepancy between β_4^C and β_4^N; this tendency, for $|\beta_4^C| > |\beta_4^N|$, has been observed[3,5,6] for many other transitional nuclei.

B. Transitions to members of the "$K = 2$" band

One of the principal motivations for performing this experiment was to deduce the sign of the $E2$ interference term $P_3 = M_{02}M_{02'}M_{22'}$ [$M_{JJ'} = -\langle J^\pi \| M(E2) \| J^{\pi'} \rangle$]. It has recently been shown[7] that $P_3 < 0$ for ^{194}Pt; this result was completely unexpected since, for any simple collective model, one expects $P_3 > 0$ if the intrinsic nuclear shape is oblate[16] (i.e., if $M_{22} < 0$). In the analysis of the second 2^+ state, the second 4^+ state was also included since it was found to have significant excitation strength and is expected to be a member of the same band as the second 2^+ state.

The coupled-channels calculations were performed with 0^+-2^+-$2^{+'}$-$4^{+'}$ coupling and the same deformations as shown in Table II. The matrix elements M_{02} and M_{22} used were the same as described in Sec. IV A. The reorientation matrix element for the second 2^+ state was assumed to be equal and opposite that of the first 2^+ state. This is expected if the second 2^+ state is a simple $K = 2$ state. (Here, too, the results are relatively insensitive to this assumption.) Fortunately, the magnitudes of the matrix elements connecting the $2^{+'}$ state to the 0^+ and 2^+ states are rather precisely known, the ratio $M_{02'}/M_{02}$ from the recent Coulomb-excitation measurements of Ronningen *et al.*,[14] and the ratio $M_{22'}/M_{02'}$ from the $2^{+'}$ γ-decay branching ratio[17] (incorporating the $E2/M1$ mixing ratio[18] for the $2^{+'} \to 2^+$ γ-decay); these were not adjusted in the calculations. Less is known about matrix elements for the $4^{+'}$ state. The most intense γ ray from the decay of this state is to the $2^{+'}$ state; intensities of the branches to the 2^+ and 4^+ states are smaller by factors of 0.07 and 0.15, respectively. Our calculations have therefore been done assuming $M_{24'} = 0$. The magnitude of $M_{2'4'}$ was estimated assuming the $2^{+'}$ and $4^{+'}$ states to be members of a simple $K = 2$ band with the same moment of inertia as the ground-state band. The reorientation matrix element for the $4^{+'}$ state was taken to be zero. The relative $L = 2$ matrix elements used in the calculations are shown in Table

TABLE III. Relative $E2$ matrix elements $M_{JJ'} = -\langle J^\pi \| M(E2) \| J^{\pi'} \rangle$ used in calculation for the "$K = 2$" band.

J/J'	0^+	2^+	$2^{+'}$	$4^{+'}$
0^+	0	1	−0.083	0
2^+	1	−0.598	1.155	0
$2^{+'}$	−0.083	1.155	0.598	2.739
$4^{+'}$	0	0	2.739	0

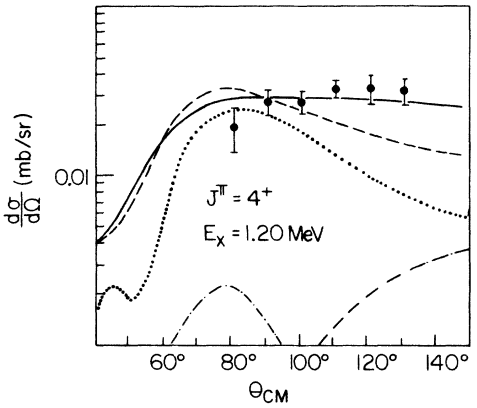

FIG. 3. Data and coupled-channels fits for the second 4^+ state. The various calculations are described in Sec. IV B of the text.

III.

Initial calculations showed, quite unambiguously, that the data for the $2^{+\prime}$ state could be satisfactorily fitted only if $P_3 < 0$. Using the relative matrix elements of Table III and assuming no direct $L=4$ excitation of the $4^{+\prime}$ state, the predicted cross section for the $4^{+\prime}$ state is approximately an order of magnitude smaller than the data as shown by the dot-dash curve in Fig. 3. The sign and magnitude of an assumed $0^+ \rightarrow 4^{+\prime}$ matrix element were then varied in an attempt to fit the data. It was found that, even though the indirect amplitude (involving two-step $0^+ \rightarrow 2^{+\prime} \rightarrow 4^{+\prime}$ and three-step $0^+ \rightarrow 2^+ \rightarrow 2^{+\prime} \rightarrow 4^{+\prime}$ excitations) is small, it interferes effectively with the direct amplitude so that the relative sign of $M_{04\prime} = +\langle 0^+ \| M(E4) \| 4^{+\prime} \rangle$ can be determined. This is shown by the full-drawn and dotted curves in Fig. 3 which are for $M_{04\prime} = +0.34\ e\,b^2$ and $M_{04\prime} = -0.20\ e\,b^2$, respectively. The isotropic nature of the data is best fitted for $M_{04\prime} > 0$. It should be noted, however, that the sign of $M_{04\prime}$ is meaningful only in relation to the signs of the pertinent $E2$ matrix elements ($M_{02}, M_{02\prime}, M_{22\prime}, M_{2'4\prime}$) and that there is uncertainty in its magnitude due to the unknown magnitude of $M_{2'4\prime}$.

It is interesting that $B(E4; 0^+ \rightarrow 4^{+\prime})$ is nearly 3 times larger than $B(E4; 0^+ \rightarrow 4^+)$. This could be indicative of an important "vibrational" component in the wave function of the $4^{+\prime}$ state similar to the recent findings of Bagnell *et al.*[19] for the third 4^+ states in ^{190,192}Os.

Finally, the sensitivity to the sign of P_3 is shown in Figs. 3 and 4. The full-drawn curves are for $P_3 < 0$, the dashed curves for $P_3 > 0$ (both with $M_{04} = +0.34\ e\,b^2$). This, as for ^{194}Pt (Ref. 7), is surprising since ^{192}Pt is expected to be intrinsically oblate. The fit to the $2^{+\prime}$ state shown in Fig. 4 is qualitatively good but not perfect. It was determined that this fit probably cannot be substantially improved by reasonable adjustment of $M_{2'2\prime}$ but could be improved by adjusting the ratio $M_{02\prime}/M_{22\prime}$. It is also possible that adjustment of the matrix element $M_{2'4\prime}$ could improve the fit since not including any $2^{+\prime}$ to $4^{+\prime}$ coupling somewhat worsens the fit.

C. Excitation of the octupole state

Calculations for the 3^- state at 1.39 MeV were done with 0^+-2^+-4^+-3^- coupling. Since, in a conventional rotational-model calculation, a 3^- state cannot be included, we approached the problem in the following way. The 0^+, 2^+, and 4^+ coupling potentials, as well as the reorientation potential for the 3^- state, were calculated by expanding the rotational-model form factors to second order in the β's. The $0^+ \rightarrow 3^-$ transition was handled using a second-order vibrational model. The $E1$ matrix elements connecting the 3^- state to the 2^+ and 4^+ states were neglected since the $3^- \rightarrow 0^+$ $E3$ γ-ray transition successfully competes with these $E1$

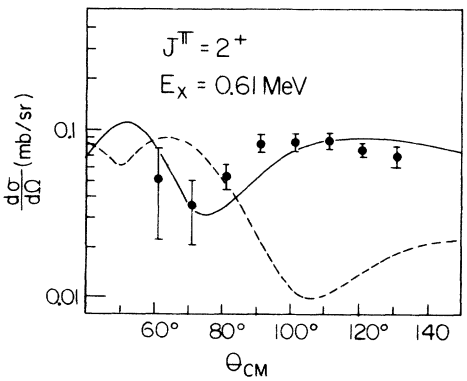

FIG. 4. Data and coupled-channels fits for the second 2^+ state. The full-drawn curve is for $P_3 < 0$, the dashed curve for $P_3 > 0$. Detailed descriptions of the calculations are given in Sec. IV B of the text.

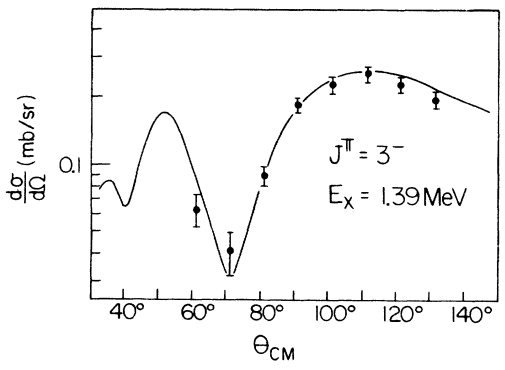

FIG. 5. Data and coupled-channels fit for the 3^- state. The calculation is described in Sec. IV C of the text.

transitions[17] suggesting the probable dominance of direct $E3$ excitations in an excitation process. The matrix element $\langle 3^- \| M(E2) \| 3^- \rangle$ was estimated, as for the other states, to have half the rotational-model value, assuming $K=0$ for the 3^- state. Since it was not felt that a reliable measurement of the Coulomb deformation parameter β_3^C could be made using our data (because of the weakness of $E3$ Coulomb excitation and the lack of smaller angle data), simple βR scaling was used to relate β_3^C to β_3^N. An excellent fit to the data, shown in Fig. 5, was achieved using $\beta_3^N=0.058$ and $\beta_3^C=0.070$. This corresponds to $B(E3; 0^+ \rightarrow 3^-)=0.19\ e^2b^3$ and is in good agreement with the Coulomb excitation measurement ($0.17 \pm 0.03\ e^2b^3$) of Ronningen *et al.*[14]

The results of the calculations are quite insensitive to the 3^- reorientation or to whether a first-order or second-order vibrational model is used for the $0^+ \rightarrow 3^-$ transition. It is important; however, that rotational-model form factors be expanded to second order so that the elastic data are well fitted. It is interesting that this second-order calculation for the 2^+ state (not shown) approximates very well the full rotational-model calculation shown in Fig. 2 but that the agreement for the 4^+ state is rather poor; this indicates that higher-order terms in the potential play an important role in describing the strong interference observed for the 4^+ state.

V. CONCLUSIONS

By measuring angular distributions for 24 MeV α-particle excitation of states in ^{192}Pt, we have determined relative signs and magnitudes of many $E2$, $E3$, and $E4$ matrix elements connecting the low-lying states. We find this technique to be much more convenient than the measurement of excitation functions.

Measurements of the quadrupole moment of the first 2^+ state and of the reduced transition rate $B(E2, 2^{+\prime} \rightarrow 4^{+\prime})$ would be useful in elucidating the nuclear structure of ^{192}Pt.

We are grateful to J. H. Hamilton for loaning us the ^{192}Pt target and to R. Kaita for valuable assistance in the acquisition of the scattering-chamber data.

---

*Work supported by NSF grant PHY 76-08788.
†Present address: Max Planck Institut fur Kernphysik, Postfach 103980, 6900 Heidelberg, Germany.
‡Work supported by a grant from USERDA.
§Operated by Union Carbide Corp. for USERDA.
¶Work supported in part by the NSF.

[1]W. Brückner, J. C. Merdinger, D. Pelte, U. Smilansky, and K. Traxel, Phys. Rev. Lett. 30, 57 (1973).
[2]I. Y. Lee, J. X. Saladin, C. Baktash, J. E. Holden, and J. O'Brien, Phys. Rev. Lett. 33, 383 (1974).
[3]W. Brückner, D. Husar, D. Pelte, U. Smilansky, and K. Traxel, Nucl. Phys. A231, 159 (1974).
[4]I. Y. Lee, J. X. Saladin, C. Baktash, J. Holden, J. O'Brien, C. Bemis, F. K. McGowan, W. T. Milner, and J. L. C. Ford, Phys. Rev. C 12, 1483 (1975).
[5]F. T. Baker, T. H. Kruse, W. Hartwig, I. Y. Lee, and J. X. Saladin, Nucl. Phys. A258, 43 (1976).
[6]F. T. Baker, A. Scott, T. H. Kruse, W. Hartwig, E. Ventura, and W. Savin, Nucl. Phys. A266, 337 (1976).
[7]F. T. Baker, A. Scott, T. H. Kruse, W. Hartwig, E. Ventura, and W. Savin, Phys. Rev. Lett. 37, 193 (1976).
[8]J. Raynal (unpublished).
[9]D. A. Goldberg and S. M. Smith, Phys. Rev. Lett. 29, 500 (1972).
[10]D. A. Goldberg, S. M. Smith, and G. F. Burdzik, Phys. Rev. C 10, 1362 (1974).
[11]N. R. Johnson, P. P. Hubert, E. Eichler, D. G. Sarantites, J. Urbon, S. W. Yates, and T. Lindblad, Phys. Rev. C 15, 1325 (1977).
[12]J. E. Glenn and J. X. Saladin, Phys. Rev. Lett. 20, 1298 (1968).
[13]L. Grodzins, B. Herskind, D. R. S. Somayajulu, and B. Skaali, Phys. Rev. Lett. 30, 453 (1973).
[14]R. M. Ronningen, R. B. Piercey, A. V. Ramayya, J. H. Hamilton, S. Raman, P. H. Stelson, and W. K. Dagenhart, Phys. Rev. C 16, 571 (1977).
[15]D. L. Hendrie, Phys. Rev. Lett. 31, 478 (1973).
[16]K. Kumar, Phys. Lett. 29B, 25 (1969).
[17]R. J. Gehrke, Nucl. Phys. A204, 26 (1973).
[18]N. A. Voinova, D. M. Kaminker, and Y. V. Sergeenkov, Nucl. Phys. A235, 123 (1974).
[19]R. D. Bagnell, Y. Tanaka, R. K. Sheline, D. G. Burke, and J. D. Sherman, Phys. Lett. 66B, 129 (1977).